



HAL
open science

Emergence of nonlinear behavior in the dynamics of ultracold bosons

Benoit Vermersch, Jean Claude Garreau

► **To cite this version:**

Benoit Vermersch, Jean Claude Garreau. Emergence of nonlinear behavior in the dynamics of ultracold bosons. *Physical Review A: Atomic, molecular, and optical physics* [1990-2015], 2015, 91, pp.043603. 10.1103/PhysRevA.91.043603 . hal-01110392

HAL Id: hal-01110392

<https://hal.science/hal-01110392>

Submitted on 28 Jan 2015

HAL is a multi-disciplinary open access archive for the deposit and dissemination of scientific research documents, whether they are published or not. The documents may come from teaching and research institutions in France or abroad, or from public or private research centers.

L'archive ouverte pluridisciplinaire **HAL**, est destinée au dépôt et à la diffusion de documents scientifiques de niveau recherche, publiés ou non, émanant des établissements d'enseignement et de recherche français ou étrangers, des laboratoires publics ou privés.

Emergence of nonlinear behavior in the dynamics of ultracold bosons

Benoît Vermersch^{1,*} and Jean Claude Garreau¹

¹*Laboratoire de Physique des Lasers, Atomes et Molécules,
Université Lille 1 Sciences et Technologies, CNRS; F-59655 Villeneuve d'Ascq Cedex, France*

We study the evolution of a system of interacting ultracold bosons, which presents nonlinear, chaotic, behaviors in the limit of very large number of particles. Using the spectral entropy as an indicator of chaos and three different numerical approaches : Exact diagonalization, truncated Husimi method and mean-field (Gross-Pitaevskii) approximation, we put into evidence the destructive impact of quantum noise on the emergence of the nonlinear dynamics.

PACS numbers: 03.75.Lm, 05.45.a, 03.75.Kk

I. INTRODUCTION

Ultracold atoms are clean, controllable, highly flexible experimental systems, that can often be modeled from first principles. For such reasons they have become in recent years a preferred testing ground for quantum many-body effects [1]. A particularly interesting example is the emergence of chaotic behaviors in quantum systems : The Schrödinger equation is linear and hence cannot display chaotic behavior in the classical sense (i.e. chaos associated to a sensitivity to initial conditions), however, the classical world very often display chaos. Bose-Einstein condensates can be produced in laboratories at mesoscopic sizes (up to 10^8 atoms) [2] in intrinsically quantum-coherent states, they are thus ideal systems for the study of the transition from quantum to classical behavior, and, in particular, the emergence of chaotic behaviors. The corresponding quantum many-body problem (with binary contact interactions) can be treated by decomposing the matter-wave field $\hat{\psi}$ in a macroscopic part describing a single particle wave function $\psi(x, t)$, called “condensed fraction”, plus a fluctuating quantum field corresponding to the excitations of the matter-wave field. The wave function $\psi(x, t)$ obeys the well-known Gross-Pitaevskii equation (GPE), which includes a *nonlinear* term [3–5] :

$$i\hbar \frac{\partial \psi(x, t)}{\partial t} = \left(H_1 + gN |\psi(x, t)|^2 \right) \psi(x, t), \quad (1)$$

where g is the nonlinear parameter proportional to the s -wave scattering length, N is the number of particles and H_1 is the one-particle Hamiltonian. The nonlinear term models the “mean effect” of particle-particle interactions, and is simply proportional to the spatial probability density $|\psi(x, t)|^2$ [26]. Replacing the many-body operator $\hat{\psi}$ by a single-particle wave function ψ which leads to the effective equation (1) implies neglecting quantum fluctuation, but preserves the long-range order supposed to be

an essential property of condensates. It turns out that in a large variety of interesting situations this rather rough approach gives a very good description of the condensate dynamics [3]. It can nevertheless be surprising that a linear exact problem can be accurately modeled by a nonlinear effective equation which may present a qualitatively different dynamics (e.g. sensitivity to initial conditions and chaos). The mean-field approximation hides the “microscopic” origin of the nonlinearity, and one is left with a situation similar to that encountered in statistical physics : The macroscopic dynamics of a gas can present qualitatively different characteristics (e.g. irreversibility) from the microscopic dynamics of individual molecules (which is reversible). The averaging over the microscopic dynamics leads to a loss of symmetry and to a qualitatively different behavior in the macroscopic scale. One can speculate that the nonlinear behavior of a condensate arises in an analog way : Averaging over the microscopic (quantum) dynamics produces a qualitatively different behavior. A particularly spectacular manifestation of this is the “quasiclassical” chaos that can appear in the dynamics of a condensate [6–10], that is, chaos related to sensitivity to initial conditions. In the present work, we will use a simple model displaying quasiclassical chaos in the mean-field approximation and will compare it to the solutions of the many-body problem. By adequately choosing the representation of the dynamics we will show that one can observe “traces” of the quasiclassical chaos in the behavior of the many-body system even with a limited number of atoms.

II. THE MODEL

The toy model used here consists in a ultracold boson gas placed in an accelerated (or tilted) optical potential [11, 12] corresponding to the single-particle Hamiltonian

$$H_1 = -\frac{1}{\pi^2} \frac{\partial^2}{\partial x^2} + V_0 \cos(2\pi x) + Fx \quad (2)$$

where we used normalized units [6] such that the lattice constant of the periodic part of the potential is 1, energies are measured in units of the so-called recoil energy

*Present Address : Institute for Quantum Optics and Quantum Information of the Austrian Academy of Sciences, A-6020 Innsbruck, Austria

($\hbar\omega_r = \hbar^2 k_L^2 / 2M$, with $k_L = \pi/d$ where d is the lattice constant of the periodic part of the potential and M is the mass of the atoms) and we have set $\hbar = 1$. In presence of interactions, a nonlinear term $g |\psi(x, t)|^2$ is added to the above Hamiltonian leading to Eq. (1). We confine the dynamics to three adjacent sites $s = -1, 0, 1$ placed at $x = -1, 0, 1$ with Dirichlet boundary conditions [27] and restrict the dynamics to the lowest band of the system; one can then write the solution of Eq. (2) in the form

$$\psi(x, t) = c_{-1} e^{iFt} w(x+1) + c_0 w(x) + c_1 e^{-iFt} w(x-1) \quad (3)$$

where $w(x)$ is the Wannier-Stark function [eigenstate of (2)] of the fundamental ladder [28] associated to the $x = 0$ site [13]. In the case $g \neq 0$, we keep the above form, but we let the coefficients c_s depend on time. Then, inserting Eq. (3) in Eq. (1) one obtains a set of coupled differential equations that can be integrated numerically :

$$i\dot{c}_s = Fsc_s + UN|c_s|^2 c_s + J_{\pm} N (2|c_s|^2 c_{s\pm 1} + |c_{s\mp 1}|^2 c_{s\mp 1} + c_{s\pm 1}^* c_s^2) \quad (4)$$

with $c_{-2} = c_2 = 0$. The first term is simply the energy of site s , the second term [with $U = g \int dx w^4(x)$] accounts for interactions of particles at the same site, and the two last terms correspond to the exchange of particles between neighbor sites, with [29]

$$J_+ = g \int dx w^3(x) w(x+1) \\ J_- = g \int dx w(x) w^3(x+1). \quad (5)$$

It is useful to write the wave function components as amplitude-phase variables, defined by $c_s = \sqrt{I_s} e^{i\theta_s}$.

The dynamics of such system has been studied in previous works [6, 8, 14, 15], where it was in particular showed that quasiclassical chaos in the above system has the structure prescribed by the Kolmogorov-Arnold-Moser theorem, which becomes apparent in a Poincaré section of the dynamics, Fig. 1a. We represented in Fig. 1b the same dynamics described in terms of the spectral entropy S . Given a dynamical function $f(t \in [0, t_{\max}])$ (e.g. the average position $\langle x \rangle(t)$), the spectral entropy is related to the power spectrum $\tilde{F}(\nu)$ of $f(t)$ by

$$S = -\frac{1}{\ln n_{\nu}} \sum_{\nu} \tilde{F}(\nu) \ln \tilde{F}(\nu),$$

where $n_{\nu} = 1 + t_{\max}/\delta t$ is the number of frequency components of $f(t)$ (with δt the corresponding resolution). Roughly speaking, the spectral entropy gives the number of significant frequency components present in the spectrum, and is thus a good indicator of (quasi)classical chaos. The aim of the present work, is to understand how the (linear) dynamics of the exact many-body problem can approach the (quasiclassical) chaotic behavior observed in Fig. 1.

III. NUMERICAL APPROACHES

The exact many-body problem can be described by the Bose-Hubbard Hamiltonian [4, 16, 17]. The single-particle Hamiltonian corresponds to Eq. (2), whereas bi-nary atom-atom contact interactions arise from a term $(g/2) \int dx \hat{\psi}^\dagger(x) \hat{\psi}^\dagger(x) \hat{\psi}(x) \hat{\psi}(x)$ where $\hat{\psi}(x)$ is the matter-wave field, which is expanded in the Wannier-Stark basis $\hat{\psi} = \sum_s w(x-s) a_s$ where a_s is the boson annihilation operator for the site s . This leads to a Bose-Hubbard Hamiltonian

$$H_{BH} = \sum_s [Fsn_s + \frac{U}{2} n_s(n_s - 1) + (J_+ a_s^\dagger a_{s+1} n_s + J_- a_s^\dagger a_{s-1} n_s + \text{h.c.})] \quad (6)$$

where $n_s = a_s^\dagger a_s$ is the number operator for site s . Note that the two “kinetic energy” terms on the second line are different from those of the usual Bose-Hubbard Hamiltonian as, contrary to Wannier functions of a periodic potential, Wannier-Stark functions are *eigenstates* of the one-particle Hamiltonian Eq. (2). Transport here is due to *interactions* between neighbor sites, not to tunnel effect, and is thus proportional to the interaction strength g [cf. Eq. (5)]. One can convince oneself that the Bose-Hubbard Hamiltonian describes the many-body Wannier-Stark problem by noticing that the mean-field approximation which consists in replacing the operators a_s by c-numbers c_s leads to a classical Hamiltonian whose equations of motions correspond to the GPE, Eq.(4). In the following, we will compare the solution of the many-body Schrödinger equation

$$i\hbar \frac{\partial |\psi_{BH}\rangle}{\partial t} = H_{BH} |\psi_{BH}\rangle, \quad (7)$$

to the solution of Eq. (4). It is challenging to directly diagonalize Eq. (6) which is of dimension $(N+1)(N+2)/2 \sim N^2$ for atom numbers N larger than a few tens, so we used the so-called “Lanczos diagonalization” (LD) [18–20], which consists in using a truncated many-body evolution operator over a short time interval dt :

$$U(dt) = \sum_{n=0}^{n_K} \frac{(-iH_{BH}dt)^n}{n!}. \quad (8)$$

In the Lanczos scheme, in order to evolve the wave function $|\psi_{BH}(t)\rangle$ during dt one first builds an orthonormal basis $|l_1\rangle, \dots, |l_{n_K}\rangle$ of the subspace spanned by n_K “Krylov vectors” defined as $|\psi_{BH}(t)\rangle, H|\psi_{BH}(t)\rangle, H^2|\psi_{BH}(t)\rangle, \dots, H^{n_K}|\psi_{BH}(t)\rangle$. The resulting tridiagonal Hamiltonian of dimension $n_K \sim 10 - 20 \ll N^2$ can be then diagonalized to obtain the Lanczos eigenvectors $|\nu_1\rangle, \dots, |\nu_{n_K}\rangle$ and eigenvalues $\alpha_1, \dots, \alpha_{n_K}$. The propagation of the wave function is then approximated as :

$$|\psi_{BH}(t+dt)\rangle = \sum_{i=1}^{n_K} \langle \nu_i | \psi_{BH}(t) \rangle e^{-i\alpha_i dt} |\nu_i\rangle.$$

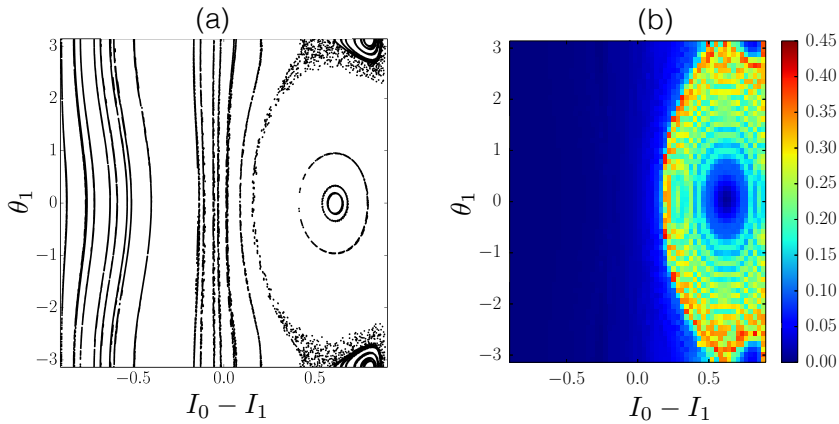


FIGURE 1: Quasiclassical chaos in a tilted lattice, obtained by integrating the Gross-Pitaevskii equation (4). (a) Poincaré section corresponding to $I_{-1} = 0.1$, $\theta_0 - \theta_{-1} = 0$. (b) Spectral entropy calculated between $t = 0$ and $t = 800$. Parameters are $V_0 = 5$, $F = 0.25$, $gN = 0.2$.

As the error in this approximation can be controlled by adjusting the time step dt , the Lanczos procedure is considered as an “exact diagonalization” technique. Each time step implies the diagonalization of a $n_K \times n_K$ matrix thus the method is only interesting if $n_K \ll N^2$. The Lanczos procedure allows us to treat the many-body problem with atom numbers $N \lesssim 500$ in reasonable computer times.

Describing the system by a set of complex numbers c_s instead of quantum operators a_s , the GPE potentially neglects two important effects : (i) quantum noise, i.e the quantum fluctuations around the expectation value of a_s (ii) quantum interferences, the fact that two different trajectories can interfere [30]. The truncated Husimi method (THM) allows one to reinsert quantum noise in a GPE description by propagating independently sets of initial conditions whose distribution reflects the quantum noise. However, the THM neglects quantum interference effects that may occur between the different trajectories and is thus an intermediary approach between the GPE and the exact solution of the many-body system particularly suited to identify the role of the quantum noise [10, 21, 22]. One thus needs to choose a rule relating the complex variables $\{c'_s\}$ serving as initials conditions to the GPE to the many-body problem, i.e to choose a family of many-body states able to connect a many-body state $|\Omega(\{c_s\})\rangle$ and the corresponding set of GPE initial conditions $\{c'_s\}$. With M sites ($M = 3$ in this work), one can choose the so-called $SU(M)$ coherent states [23] with finite total number of atoms N , which are defined, in the Fock basis, as

$$|\Omega(\{c_s\})\rangle = \sqrt{N!} \sum_{n_1 + \dots + n_M = N} \prod_s \frac{c_s^{n_s}}{\sqrt{n_s!}} |n_1, \dots, n_M\rangle$$

with $\sum_s |c_s|^2 = 1$. The advantage of $SU(M)$ states, as compared to the usual Glauber coherent states, is that the *total* number of atoms N is fixed : $\langle (\hat{N} - \langle \hat{N} \rangle)^2 \rangle =$

0, with $\hat{N} = \sum_s n_s$, which is a situation closer to the that encountered in a real experiment. We then need to choose a quantity to characterize the quantum noise in the system. In this work we use the Husimi function Q_Ω which, given a coherent state $|\Omega(\{c_s\})\rangle$, is simply defined as its projection over all possible states : $Q_\Omega(\{c'_s\}) = |\langle \Omega'(\{c'_s\}) | \Omega(\{c_s\}) \rangle|^2$. The width of this function decreases as $N^{-1/2}$ and thus gives a good representation of the quantum noise. For a given initial many-body state $|\Omega\{c_s\}\rangle$, we generate the corresponding *distribution* of one-particle initial conditions $D(c_s) \equiv \{c'_s\}$ which mimics the Husimi representation of the $|\Omega\{c_s\}\rangle$. Each of these states is then propagated independently according to the GPE and observables are obtained by averaging over the distribution of final states. For large enough N , the width of the Husimi distribution tends to 0 and one recovers the results of the GPE. Hence, the THM allows one to use the GPE to simulate the evolution of not so large number of atoms (including quantum noise but not interference effects), and it turns out to be a convenient tool to study of the emergence of chaos in our system as the number of atoms increases.

IV. EMERGENCE OF QUASICLASSICAL CHAOS

We compare in Fig. 2 the time evolution of the system – represented here by the average position of the wave packet – calculated according to the different methods described in sec. III, for a small $N = 30$ [plot (a)] and a larger (but not large) $N = 500$ [plot (b)] number of atoms. In order to have a pertinent comparison with the GPE, gN is the same for all simulations. The GPE calculation displays a clear irregular behavior associated to the presence of quasiclassical chaos. No such behavior is observed for $N = 30$ atoms either with the LD or the THM. In plot (b), with $N = 500$, one sees that the GPE

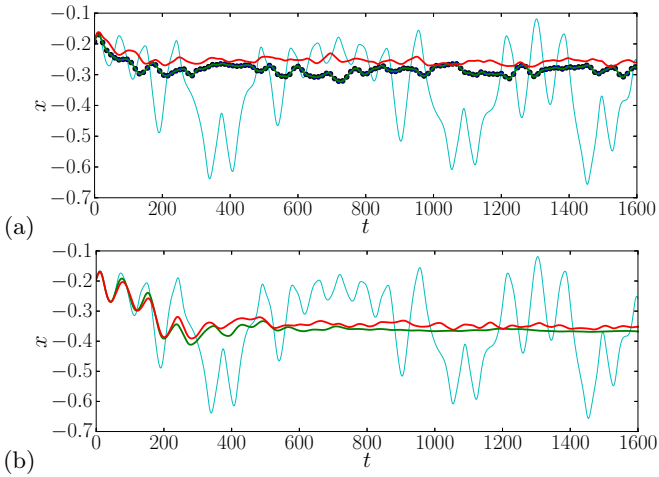


FIGURE 2: Evolution of the average position of a wave packet calculated with different methods : Gross-Pitaevskii equation (cyan), Lanczos diagonalization (green), and the truncated Husimi method (red), for (a) $N = 30$ and (b) $N = 500$. In panel (a), we also represented by blue circles the result obtained by direct diagonalization of the full many-body problem, which is in perfect agreement with the result of the Lanczos method, illustrating the accuracy of the later. The initial state is a $SU(3)$ coherent state with $c_{-1} = \sqrt{0.5}$, $c_0 = \sqrt{0.25}$ and $c_1 = i\sqrt{0.25}$. Other parameters are $gN = 0.2$, $V_0 = 7$, $F = 0.1$.

result “sticks” to the many-body calculations for times $t \lesssim 150$, and that the many-body calculations even display the first oscillations observed in the GPE evolution.

In order to observe the emergence of quasiclassical chaos as the number of particles increases, we calculated the spectral entropy for a complete set of initial $SU(3)$ states using both LD and THM. The width of the Husimi function corresponding to a given initial condition is determined, and we assume that for any initial condition $\{c_s\}$, the Husimi function can be approximated by a square distribution with same width centered around $\{c_s\}$. We checked numerically that this approximation has no impact on our results. Figure 3 compares the distribution of the spectral entropy computed by LD and by the THM for $N = 30$ and $N = 400$ atoms, and shows that not only the results become more similar when the atom number increases, but also that the characteristic features observed in the quasiclassical Poincaré section Fig. 1a tend to emerge (this trend is confirmed for intermediate atom numbers). These results show that THM provides a good representation of the exact many-body behavior for large atom numbers and can advantageously be used for comparisons with the quasiclassical behavior.

In figure 4 we present a calculation of the variance of the wave packet position – which is an indication of the erratic character of the dynamics, that is quasiclassical chaos – by the three methods and for $N = 30$ (top row) and $N = 400$ (bottom row). The GPE picture (first column) is obviously independent of the atom number (provided gN is constant). Both LD (center column) and

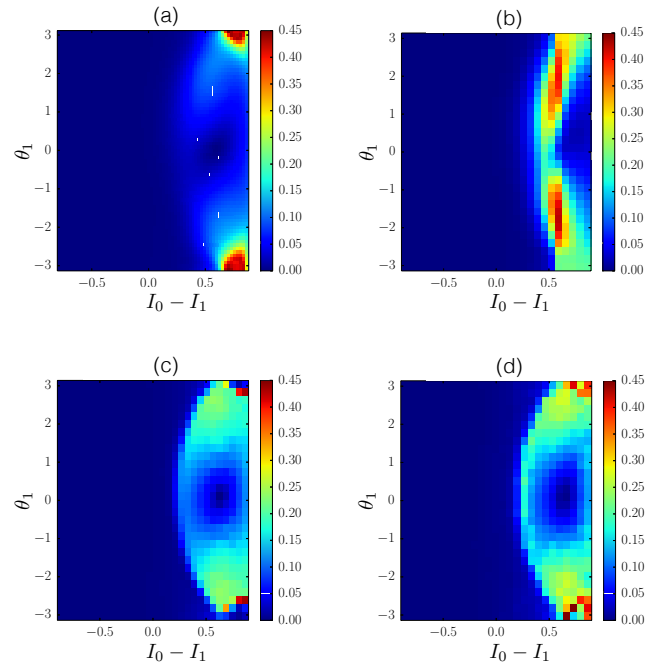


FIGURE 3: Spectral entropy distribution in phase space obtained by LD (left column) and by THM (right column) with $N = 30$ (top row) $N = 400$ (bottom row) and same parameters as Fig. 1. When N increases, the THM provides a quite good representation of the mean-field behavior for large N , and the phase-space structure of the many-body problem becomes similar to the Poincaré section obtained from the GPE, plot (a) of Fig. 1.

THM (right column) instead show a clear dependence in N and are rather different, both in shape as in the amplitude, from the GPE result, which shows that quasiclassical chaos is not fully developed for such atom numbers. However, one can see however that the higher the number of atoms the closer the result is from the one obtained with GPE. The amplitude of the variances increases by a factor 2 for THM and by a factor 3.8 for the LD when the number of atoms is changed from 30 to 400, and the surface of the chaotic zones (in yellow and red) also increases significantly. Thus, even if the atom numbers considered here are clearly too small to allow a definite conclusion, one can reasonably expect a much better convergence with the GPE for larger values of N .

V. CONCLUSION

In conclusion, we showed that the dynamics exhibited by the many-body problem as described by both exact diagonalization and the truncated Husimi method tends to converge to the quasiclassical chaos displayed by the mean-field approximation as the atom number increases. Our result suggests the existence of a “nonlinear characteristic time” increasing with some (monotonous) function of N , during which the prediction of the mean-field ap-

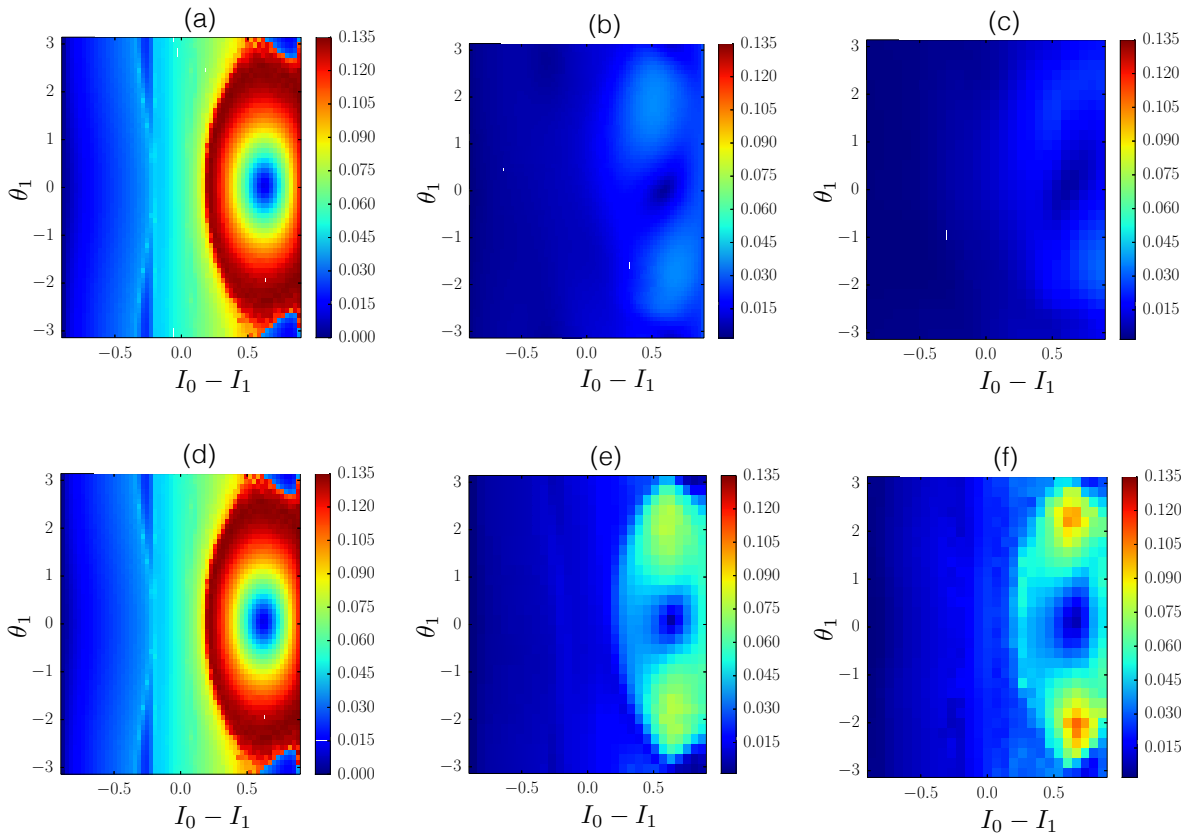


Figure 4: Variance of the wave packet position calculated between $t = 0$ and $t = 800$ from the GPE (left column), LD (center column), and THM (right column) with $N = 30$ (top row) and $N = 400$ (bottom row) and the same parameters as Fig. 1.

proximation and of the exact many-body problem agree. One may conjecture that this time is related to the typical time for particle number fluctuations to affect significantly the dynamics, but we are presently unable to give a verifiable estimation of such time. In particular, THM appears to approach very well the exact dynamics, which suggests that the essential effect leading to the emergence of quasiclassical chaos as the number of particles increases is the reduction of quantum noise. It would be interesting to analyze the influence of quantum interferences and diffusion as done e.g. by Carvalho *et al.* [24], who compared the phase space structure of the classical chaotic *one-body* delta-kicked harmonic oscillator to the Wigner representation of its quantum counterpart, and showed that both decoherence and classical diffusion lead to a similarity of the two representations. Weiss and Teichmann [25], using a *many-body* system (with $N = 1000$) slightly different from ours, attributed the observed differences between the mean-field and the many-body dynamics to the existence of entanglement in the many-body problem, and showed that these differences are reduced if decoherence is added to the

system. The present work sheds a different light on the problem of the quantum-classical transition in a system displaying quasiclassical chaos, suggesting the quantum noise is the main cause of the differences. In order to reach more definitive conclusions, however, simulations of the many-body problem with atom numbers larger by (at least) one order of magnitude would be necessary. This is a fascinating yet challenging goal for future work.

Acknowledgments

Laboratoire de Physique des Lasers, Atomes et Molécules is UMR 8523 of CNRS. Work partially supported by Agence Nationale de la Recherche (grants LAKRIDI ANR-11-BS04-0003,2 K-BEC ANR-13-BS04-0001-01) and the Labex CEMPI (ANR-11-LABX-0007-01). JCG thanks the Max-Planck Institute for the Physics of Complex Systems, Dresden, for support in the framework of the Advanced Study Group on Optical Rare Events.

[1] I. Bloch, J. Dalibard, and W. Zwerger, *Rev. Mod. Phys.* **80**, 885 (2008).

[2] E. W. Streed, A. P. Chikkatur, T. L. Gustavson, M. Boyd,

- Y. Torii, D. Schneble, G. K. Campbell, D. E. Pritchard, and W. Ketterle, *Rev. Sci. Instrum.* **77** (2006).
- [3] F. Dalfovo, S. Giorgini, L. Pitaevskii, and S. Stringari, *Rev. Mod. Phys.* **71**, 463 (1999).
- [4] C. Cohen-Tannoudji and D. Guéry-Odelin, *Advances In Atomic Physics: An Overview* (World Scientific Publishing, Singapore, 2011).
- [5] C. J. Pethick and H. Smith, *Bose-Einstein Condensation in Dilute Gases* (Cambridge University Press, Cambridge, UK, 2008), 2nd ed.
- [6] Q. Thommen, J. C. Garreau, and V. Zehnlé, *Phys. Rev. Lett.* **91**, 210405 (2003).
- [7] G. P. Berman, F. Borgonovi, F. M. Izrailev, and A. Smerzi, *Phys. Rev. Lett.* **92**, 030404 (2004).
- [8] M. Lepers, V. Zehnlé, and J. C. Garreau, *Phys. Rev. Lett.* **101**, 144103 (2008).
- [9] L. Fallani, L. De Sarlo, J. E. Lye, M. Modugno, R. Saers, C. Fort, and M. Inguscio, *Phys. Rev. Lett.* **93**, 140406 (2004).
- [10] F. Trimborn, D. Witthaut, and H. J. Korsch, *Phys. Rev. A* **79**, 013608 (2009).
- [11] M. Ben Dahan, E. Peik, J. Reichel, Y. Castin, and C. Salomon, *Phys. Rev. Lett.* **76**, 4508 (1996).
- [12] S. R. Wilkinson, C. F. Bharucha, K. W. Madison, Q. Niu, and M. G. Raizen, *Phys. Rev. Lett.* **76**, 4512 (1996).
- [13] Q. Thommen, J. C. Garreau, and V. Zehnlé, *Phys. Rev. A* **65**, 053406 (2002).
- [14] A. R. Kolovsky, H. J. Korsch, and E.-M. Graefe, *Phys. Rev. A* **80**, 023617 (2009).
- [15] A. R. Kolovsky, E. A. Gómez, and H. J. Korsch, *Phys. Rev. A* **81**, 025603 (2010).
- [16] D. Jaksch, C. Bruder, J. I. Cirac, C. W. Gardiner, and P. Zoller, *Phys. Rev. Lett.* **81**, 3108 (1998).
- [17] P. Meystre, *Atom Optics* (Springer-Verlag, Berlin, Germany, 2001).
- [18] C. Lanczos, *J. Res. Nat. Bur. Stand.* **45**, 255 (2014).
- [19] S. R. Manmana, A. Muramatsu, and R. M. Noack, *AIP Conf. Proc.* **789**, 269 (2005).
- [20] G. Carleo, F. Becca, M. Schiró, and M. Fabrizio, *Sci. Rep.* **2** (2014).
- [21] A. Sinatra, C. Lobo, and Y. Castin, *J. Phys. B : At. Mol. Opt. Phys.* **35**, 3599 (2002).
- [22] F. Trimborn, D. Witthaut, and H. J. Korsch, *Phys. Rev. A* **77**, 043631 (2008).
- [23] W.-M. Zhang, D. H. Feng, and R. Gilmore, *Rev. Mod. Phys.* **62**, 867 (1990).
- [24] A. R. R. Carvalho, R. L. de Matos Filho, and L. Davidovich, *Phys. Rev. E* **70**, 026211 (2004).
- [25] C. Weiss and N. Teichmann, *Phys. Rev. Lett.* **100**, 140408 (2008).
- [26] The form (1) of the GPE corresponds to the normalization choice $\int dx |\psi|^2 = 1$.
- [27] This is not an unphysical assumption, for if g is not too small, the nonlinear term decouples the dynamics of populated wells from the others (a phenomenon called *self-trapping*) and the population can stay confined in these three wells for quite long times.
- [28] As long as $gN \int w^4(x) dx \ll V_0$ the coupling to higher ladders is negligible.
- [29] We work in the first-neighbors approximation which is valid if $V_0/F \gtrsim 5$. In this limit, we can neglect terms proportional to $\int dx w^2(x) w^2(x+1) \ll \int dx w^3(x) w(x+1)$.
- [30] We use here the language of second quantization which means that quantum interference is described by GPE only at the single particle level (e.g. it displays nonlinear Bloch Oscillations) - that is, interference governed by the phase of the c_s themselves.